Nonlinear dynamics in low permittivity media: the impact of losses

M. A. Vincenti,[1,*] D. de Ceglia,[1] and M. Scalora[2]

[1]*National Research Council – AMRDEC, Charles M. Bowden Research Lab, Redstone Arsenal – AL, 35898, USA*
[2]*Charles M. Bowden Research Lab, AMRDEC, US Army RDECOM, Redstone Arsenal - AL, 35898, USA*
[*]*maria.vincenti@us.army.mil*

Abstract. Slabs of materials with near-zero permittivity display enhanced nonlinear processes. We show that field enhancement due to the continuity of the longitudinal component of the displacement field drastically enhances harmonic generation. We investigate the impact of losses with and without bulk nonlinearities and demonstrate that in the latter scenario surface, magnetic and quadrupolar nonlinear sources cannot always be ignored.

OCIS Codes: (190.2620) Harmonic generation and mixing; (190.4350) Nonlinear optics at surfaces.

References and links

1. J. Brown, "Artificial dielectrics having refractive indices less than unity," IEE Proc. Part IV Inst. Monogr. **100**, 51–62 (1953).
2. W. Rotman, "Plasma simulation by artificial dielectrics and parallel-plate media," IRE Trans. Antennas Propag. **10**(1), 82–95 (1962).
3. S. Enoch, G. Tayeb, P. Sabouroux, N. Guérin, and P. Vincent, "A metamaterial for directive emission," Phys. Rev. Lett. **89**(21), 213902 (2002).
4. G. Lovat, P. Burghignoli, F. Capolino, D. R. Jackson, and D. R. Wilton, "Analysis of directive radiation from a line source in a metamaterial slab with low permittivity," IEEE Trans. Antennas Propag. **54**(3), 1017–1030 (2006).
5. M. Silveirinha and N. Engheta, "Tunneling of electromagnetic energy through subwavelength channels and bends using ε-near-zero materials," Phys. Rev. Lett. **97**(15), 157403 (2006).
6. S. Campione, D. de Ceglia, M. A. Vincenti, M. Scalora, and F. Capolino, "Electric field enhancement in ε-near-zero slabs under TM-polarized oblique incidence," Phys. Rev. B **87**(3), 035120 (2013).
7. D. A. Powell, A. Alù, B. Edwards, A. Vakil, Y. S. Kivshar, and N. Engheta, "Nonlinear control of tunneling through an epsilon-near-zero channel," Phys. Rev. B **79**(24), 245135 (2009).
8. M. A. Vincenti, D. de Ceglia, A. Ciattoni, and M. Scalora, "Singularity-driven second- and third-harmonic generation at ε-near-zero crossing points," Phys. Rev. A **84**(6), 063826 (2011).
9. A. Ciattoni and E. Spinozzi, "Efficient second-harmonic generation in micrometer-thick slabs with indefinite permittivity," Phys. Rev. A **85**(4), 043806 (2012).
10. M. A. Vincenti, S. Campione, D. de Ceglia, F. Capolino, and M. Scalora, "Gain-assisted harmonic generation in near-zero permittivity metamaterials made of plasmonic nanoshells," New J. Phys. **14**(10), 103016 (2012).
11. A. Ciattoni, C. Rizza, and E. Palange, "Extreme nonlinear electrodynamics in metamaterials with very small linear dielectric permittivity," Phys. Rev. A **81**(4), 043839 (2010).
12. D. de Ceglia, S. Campione, M. A. Vincenti, F. Capolino, and M. Scalora, "Low-damping epsilon-near-zero slabs: Nonlinear and nonlocal optical properties," Phys. Rev. B **87**(15), 155140 (2013).
13. C. Rizza, A. Ciattoni, and E. Palange, "Two-peaked and flat-top perfect bright solitons in nonlinear metamaterials with epsilon near zero," Phys. Rev. A **83**(5), 053805 (2011).
14. E. D. Palik and G. Ghosh, *Handbook of Optical Constants of Solids* (Academic, 1998).
15. S. Campione, M. Albani, and F. Capolino, "Complex modes and near-zero permittivity in 3D arrays of plasmonic nanoshells: loss compensation using gain [Invited]," Opt. Mater. Express **1**(6), 1077–1089 (2011).
16. S. Campione and F. Capolino, "Composite material made of plasmonic nanoshells with quantum dot cores: loss-compensation and ε-near-zero physical properties," Nanotechnology **23**(23), 235703 (2012).
17. A. Ciattoni, R. Marinelli, C. Rizza, and E. Palange, "|ε|-Near-zero materials in the near-infrared," Appl. Phys. B **110**(1), 23–26 (2013).
18. S. Xiao, V. P. Drachev, A. V. Kildishev, X. Ni, U. K. Chettiar, H.-K. Yuan, and V. M. Shalaev, "Loss-free and active optical negative-index metamaterials," Nature **466**(7307), 735–738 (2010).
19. M. Scalora, M. A. Vincenti, D. de Ceglia, V. Roppo, M. Centini, N. Akozbek, and M. J. Bloemer, "Second- and third-harmonic generation in metal-based structures," Phys. Rev. A **82**(4), 043828 (2010).
20. D. T. Owens, C. Fuentes-Hernandez, J. M. Hales, J. W. Perry, and B. Kippelen, "A comprehensive analysis of the contributions to the nonlinear optical properties of thin Ag films," J. Appl. Phys. **107**(12), 123114 (2010).

#197602 - $15.00 USD Received 12 Sep 2013; revised 15 Oct 2013; accepted 16 Oct 2013; published 27 Nov 2013

21. M. A. Vincenti, D. de Ceglia, V. Roppo, and M. Scalora, "Harmonic generation in metallic, GaAs-filled nanocavities in the enhanced transmission regime at visible and UV wavelengths," Opt. Express **19**(3), 2064–2078 (2011).
22. N. N. Lepeshkin, A. Schweinsberg, G. Piredda, R. S. Bennink, and R. W. Boyd, "Enhanced Nonlinear Optical Response of One-Dimensional Metal-Dielectric Photonic Crystals," Phys. Rev. Lett. **93**(12), 123902 (2004).
23. M. Airola, Y. Liu, and S. Blair, "Second-harmonic generation from an array of sub-wavelength metal apertures," J. Opt. A **7**(2), S118–S123 (2005).
24. A. Lesuffleur, L. K. S. Kumar, and R. Gordon, "Enhanced second harmonic generation from nanoscale double-hole arrays in a gold film," Appl. Phys. Lett. **88**(26), 261104 (2006).
25. N. Rakov, F. E. Ramos, and M. Xiao, "Strong second-harmonic radiation from a thin silver film with randomly distributed small holes," J. Phys. Condens. Matter **15**(23), L349–L352 (2003).
26. T. Xu, X. Jiao, and S. Blair, "Third-harmonic generation from arrays of sub-wavelength metal apertures," Opt. Express **17**(26), 23582–23588 (2009).
27. M. Scalora, M. Vincenti, D. de Ceglia, N. Akozbek, V. Roppo, M. Bloemer, and J. Haus, "Dynamical model of harmonic generation in centrosymmetric semiconductors at visible and UV wavelengths," Phys. Rev. A **85**(5), 053809 (2012).
28. M. A. Vincenti, D. de Ceglia, J. W. Haus, and M. Scalora, "Harmonic generation in multiresonant plasma films," Phys. Rev. A **88**(4), 043812 (2013).

1. Introduction

Artificial, near-zero permittivity (NZP) materials were first predicted more than 50 years ago [1, 2]. Since then much attention has been devoted to their linear properties and applications, such as the improvement of antenna directivity [3, 4] and perfect coupling through arbitrarily shaped spatial regions [5]. In addition, the longitudinal (normal to the surface) component of an incident, TM-polarized electric field becomes singular at the interface and inside the material [6]. These materials may then be exploited for nonlinear optical processes [7] such as harmonic generation [8–10], optical bistability [11, 12], and soliton excitation [13]. All naturally occurring materials have two zero-crossing points for the real part of the permittivity in proximity of any electronic, Lorentzian resonance. The positions of the crossing points vary from the far infrared for fluorides and glasses, to the visible and ultraviolet for metals and semiconductors [14]. Absorption, usually not negligible near these resonances, limits electric field enhancement and frustrates both linear and nonlinear optical properties. For this reason solutions to mitigate losses have been discussed in the context of artificial NZPs: active materials may be introduced inside metal-based composites to tailor the electric or magnetic properties to significantly decrease absorption losses [15–18]. The inclusion of metals in artificial NZP media has additional implications due to the nonlinear response arising from symmetry breaking at the surface, the magnetic Lorentz force, inner-core electrons, convective sources, and electron gas pressure [10, 19]. Metals also display a large third-order nonlinearity that may significantly contribute to the generated signals, especially under circumstances where the electric field is dramatically enhanced [20–26].

In this paper we present a brief overview of the linear properties of slabs with NZP properties, and discuss the impact of losses on linear and nonlinear processes. We then consider a scenario where bulk nonlinearities are removed and evaluate the efficiency of harmonic generation arising only from surface, magnetic, and quadrupolar contributions. Our findings suggest that NZP materials are good candidates for low-intensity nonlinear optics, as we show that bulk nonlinearities are not necessary to achieve relatively efficient harmonic generation.

2. Linear properties of NZP materials: the impact of losses

If a monochromatic, TM-polarized plane wave impinges on an interface between a generic medium and a material with relative permittivity that tends to zero, the longitudinal component of the electric field inside the NZP material (E_z) becomes singular. This follows immediately from the condition $E_z = E_{z,0}\,\varepsilon_0/\varepsilon_{\mathrm{M}}$, where $E_{z,0}$ and ε_0 are the longitudinal component of the electric field and permittivity, respectively, in the half-space of incidence, and ε_{M} is the permittivity of the NZP medium. This condition is achieved when the angle of incidence matches the Brewster or critical angle [6]. In contrast, in slabs of finite thickness

#197602 - $15.00 USD Received 12 Sep 2013; revised 15 Oct 2013; accepted 16 Oct 2013; published 27 Nov 2013

E_z may become singular by either (i) reducing the thickness of the slab, or (ii) approaching normal incidence [6]. We first consider the linear properties of a homogenous slab of material of thickness d = 200 nm. The slab is surrounded by air and is illuminated by a TM-polarized plane wave incident at an angle ϑ_i with respect to the z-axis, with electric field and wave-vector on the x-z plane, as shown in Fig. 1(a). The slab has relative permittivity $\varepsilon_{\mathrm{M}}(\omega)$ modeled by a superposition of classical Lorentz oscillators:

$$\varepsilon_{\mathrm{M}}(\omega) = 1 - \sum_{\mathrm{j}} \frac{\omega_{\mathrm{p_j}}^2}{\omega^2 - \omega_{0\mathrm{j}}^2 + i\omega\gamma_{\mathrm{j}}}. \qquad (1)$$

The plasma frequencies are denoted by $\omega_{\mathrm{p_j}}$, γ_{j} are damping coefficients, $\omega_{0\mathrm{j}}$ are resonance frequencies, ω is the angular frequency, and $i \equiv \sqrt{-1}$. The parameters are scaled with respect to the reference angular frequency $\omega_{\mathrm{r}} = 2\pi c/1\ \mu\mathrm{m}$ and c is the speed of light in vacuum. From Eq. (1) one may infer that for each oscillator $\mathrm{Re}[\varepsilon_{\mathrm{M}}(\omega)]$ crosses zero twice at frequencies that depend on $\omega_{\mathrm{p_j}}$ and $\omega_{0\mathrm{j}}$ and γ_{j}. The values of $\mathrm{Im}[\varepsilon_{\mathrm{M}}(\omega)]$ at the crossing points differ substantially from each other, but one may safely assume that absorption is much smaller at the high-energy crossing point. For simplicity we model the slab with a single Lorentz oscillator with parameters $\omega_{\mathrm{p1}} = 0.906049\,\omega_{\mathrm{r}}$, $\omega_{01} = 0.25\,\omega_{\mathrm{r}}$, $\gamma_1 = 0.01\,\omega_{\mathrm{r}}$ that yield $\varepsilon_{\mathrm{M}} = 1.703\times10^{-7} + i0.0115$ at λ_ω = 1064 nm. The second crossing point occurs at 4 μm and will not be considered here. Transmission, reflection and absorption maps are shown in Figs. 1(b)–1(d), respectively, as functions of incident angle and wavelength.

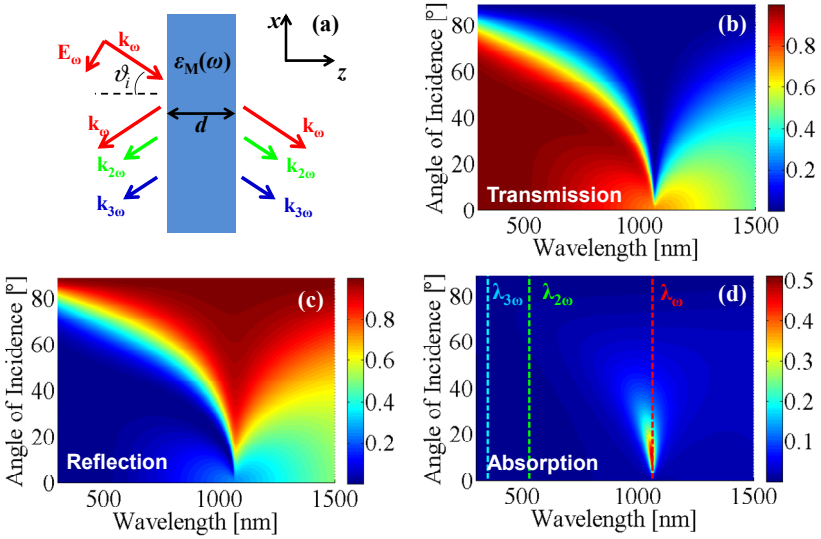

Fig. 1. (a) A TM-polarized pump impinges on a slab with thickness d and angle of incidence ϑ_i; (b) Transmission, (c) Reflection and (d) Absorption when d = 200nm. Fundamental (red, dashed line marked λ_ω), second (green, dashed line marked $\lambda_{2\omega}$) and third (blue, dashed line marked $\lambda_{3\omega}$) harmonic wavelengths are shown on the absorption map.

Transmission and reflection frequency selectivity and asymmetry depend on the slope and sign of $\mathrm{Re}[\varepsilon_{\mathrm{M}}(\omega)]$. In contrast, both angular and spectral selectivity of the slab's absorption [Fig. 1(c)] depend on $\mathrm{Im}[\varepsilon_{\mathrm{M}}(\omega)]$, which in turn depends on the damping coefficient γ_1. No

#197602 - $15.00 USD Received 12 Sep 2013; revised 15 Oct 2013; accepted 16 Oct 2013; published 27 Nov 2013

other spectral and angular features are discernible away from the pump wavelength λ_ω = 1064nm [red, dashed line in Fig. 1(d)]. Absorption is low at the second [green, dashed line marked $\lambda_{2\omega} = 2\lambda_\omega$ in Fig. 1(d)] and third harmonic wavelengths, [blue, dashed line marked $\lambda_{3\omega} = 3\lambda_\omega$ in Fig. 1(d)]. It is well-known that electric field enhancement [Fig. 2(a)] is related to the absorption profile [Fig. 1(d)] and is thus linked to the choice of damping coefficient γ_1. However, in this system absorption values depend weakly on $\mathrm{Im}[\varepsilon_M(\omega)]$: for example, we find that decreasing γ_1 by two orders of magnitude does not result in substantial decrease in maximum absorption, which is in fact proportional to the product $\mathrm{Im}[\varepsilon_M(\omega)]|\mathbf{E}|^2$. At the crossing point near λ_ω, a decreasing $\mathrm{Im}[\varepsilon_M(\omega)]$ is associated with an increasing electric field enhancement: more specifically the electric field enhancement grows proportionally to $1/\sqrt{\mathrm{Im}[\varepsilon_M(\omega)]}$. Even if absorption losses were not negligible at the pump wavelength, nonlinear optical interactions are expected to persist even for relatively large γ_1. Figure 2 shows the electric field enhancement maps for different values of γ_1 as a function of wavelength and angle of incidence.

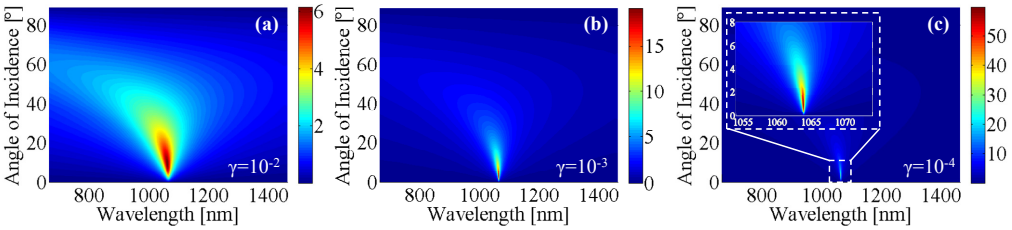

Fig. 2. Electric field enhancement [$\max\left(|E_z|/|E_{z0}|\right)$] vs. wavelength and angle of incidence for a d = 200nm thick, modeled with $\omega_{p1} = 0.906049\,\omega_r$, $\omega_{01} = 0.25\,\omega_r$ and (a) $\gamma_1 = 0.01\,\omega_r$, (b) $\gamma_1 = 0.001\,\omega_r$ and (c) $\gamma_1 = 0.0001\,\omega_r$.

3. Impact of losses on nonlinear dynamics in the presence of bulk nonlinearities

Second and third order nonlinear effects are accounted for by expressing the leading contributions of the nonlinear polarization densities in the k-direction at the second (SH) and third harmonic (TH) frequencies as $P_{2\omega,k} = \varepsilon_0 \sum_{l,m=1}^{3} \chi^{(2)}_{klm}(2\omega,\omega,\omega) E_{\omega,l} E_{\omega,m}$ and $P_{3\omega,k} = \varepsilon_0 \sum_{l,m,n=1}^{3} \chi^{(3)}_{klmn}(3\omega,\omega,\omega,\omega) E_{\omega,l} E_{\omega,m} E_{\omega,n}$, where k,l,m,n are the Cartesian axes, $\chi^{(2)}_{klm}$ and $\chi^{(3)}_{klmn}$ are the instantaneous second and third order susceptibility tensor components, respectively. We assume $\chi^{(2)}_{xxx} = \chi^{(2)}_{yyy} = \chi^{(2)}_{zzz} = 10\,\mathrm{pm/V}$, $\chi^{(3)}_{xxxx} = \chi^{(3)}_{yyyy} = \chi^{(3)}_{zzzz} = 10^{-20}\ \mathrm{m^2/V^2}$ and a continuous wave pump with irradiance $I_\omega = 100\,\mathrm{MW/cm^2}$, and evaluate SHG and THG for slabs d = 200 nm thick for different damping coefficients (Fig. 3). The total SH ($I_{2\omega}/I_\omega$) and TH ($I_{3\omega}/I_\omega$) conversion efficiencies in the undepleted pump approximation are of the order of 10^{-5} and 10^{-7} [Figs. 3(a)–3(b)] when $\gamma_1 = 0.01\,\omega_r$. SH and TH efficiencies increase by one and two orders of magnitude, respectively, if the damping coefficient is reduced to $\gamma_1 = 0.001\,\omega_r$ [Figs. 3(c) and 3(d)]. The efficiency maps resemble the field enhancement map [Figs. 2(a) and 2(b)] in spectral and angular features. The results in Fig. 3

#197602 - $15.00 USD Received 12 Sep 2013; revised 15 Oct 2013; accepted 16 Oct 2013; published 27 Nov 2013

may also be obtained using pulses 400 fs or longer for $\gamma_1 = 0.01\,\omega_r$, or at least 800 fs when $\gamma_1 = 0.001\,\omega_r$ to resolve the respective spectral features.

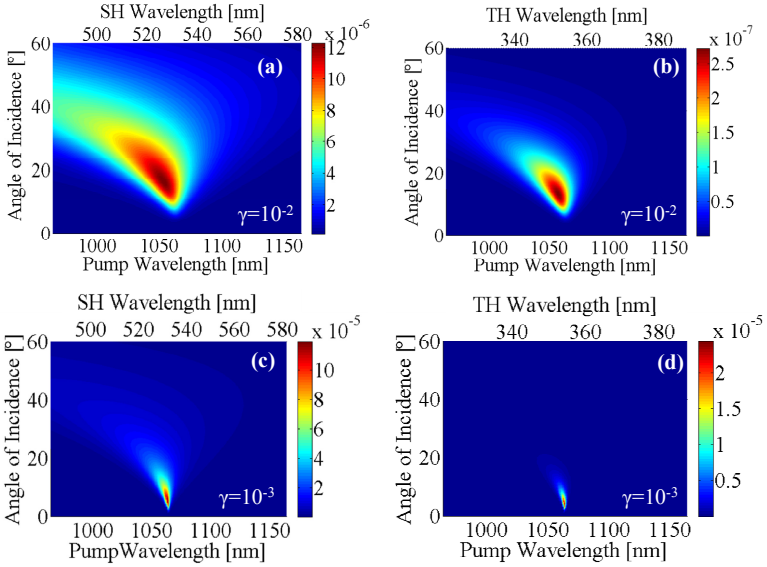

Fig. 3. Total (a) SH and (b) TH conversion efficiencies for a slab d = 200 nm thick as a function of incident angle and pump wavelength. The slab is modeled assuming $\omega_{p1} = 0.906049\,\omega_r$, $\omega_{01} = 0.25\,\omega_r$, and $\gamma_1 = 0.01\,\omega_r$. (c) and (d) same as in (a) and (b) for $\gamma_1 = 0.001\,\omega_r$.

4. Nonlinear dynamics of NZP materials in the absence of bulk nonlinearities

If $\chi^{(2)}$ and $\chi^{(3)}$ are either sufficiently small or absent, only surface, magnetic [19], and electric quadrupole sources contribute to harmonic generation. One may then write equations of motion for the polarizations at the pump, SH and TH frequencies that take into account all of the above contributions, as described in details in Ref [27]. Choosing the same two sets of oscillator parameters described in Sec. 3 one may then quantify SH and TH efficiencies and assess the role of losses. By assuming $I_\omega = 100\,\mathrm{MW/cm^2}$, 400fs pulses, and tuning the pump such that $\varepsilon_M = 1.703\times10^{-7} + i0.0115$ at λ_ω = 1064 nm, we obtain a new total SH conversion efficiency maximum of $\sim10^{-10}$ [Fig. 4(a), blue, solid line], and a vanishingly small TH efficiency maximum of $\sim10^{-19}$ when $\gamma_1 = 0.01\,\omega_r$ [Fig. 4(b), blue, solid line]. By reducing the damping coefficient to $\gamma_1 = 0.001\,\omega_r$ and increasing pulse width to at least 800fs, maximum SH and TH efficiencies are of order 10^{-9} [Fig. 4(a), red, dashed line] and 10^{-17} [Fig. 4(b), red, dashed line], respectively. For comparison, we note that the maximum SH conversion efficiency shown in Fig. 4(a) is still ~100 times larger than the SH response of a silver grating where surface plasmons or resonant cavity modes are excited [19, 21].

Another, perhaps more interesting aspect of harmonic generation occurs in multi-resonant plasma films, as recently reported [28], where the SH and/or TH signals are also tuned in spectral regions where the permittivity is close to zero. In that case the dynamics is affected by the magnitude of the near-zero effective index at the harmonic in question, boosting dramatically conversion efficiencies [28]. In Fig. 5 we plot the new conversion efficiencies that exploit the NZP condition both at the pump and SH or TH wavelengths, accomplished by introducing resonances in the oscillators as indicated in the Fig. 5 caption. Our calculations,

#197602 - $15.00 USD Received 12 Sep 2013; revised 15 Oct 2013; accepted 16 Oct 2013; published 27 Nov 2013

carried out using pulses having durations up to ~800fs to resolve the resonances for different damping coefficients, show that while SH conversion efficiency grows by an additional two orders of magnitudes to 10^{-7}, the impact of this condition is more dramatic when the NZP condition occurs for the TH frequency, producing a more than remarkable improvement of eleven orders of magnitude in THG, notwithstanding the fact that the bulk $\chi^{(3)} = 0$.

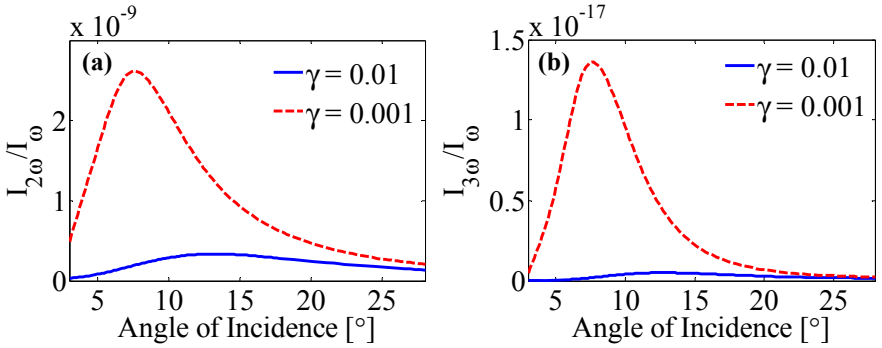

Fig. 4. (a) SH efficiency vs. angle of incidence for a slab d = 200 nm thick, modeled with $\omega_{p1} = 0.906049\,\omega_r$, $\omega_{01} = 0.25\,\omega_r$ and $\gamma_1 = 0.01\,\omega_r$ (blue, solid line) and $\gamma_1 = 0.001\,\omega_r$ (red, dashed line). (b) Same as in (a) for TH.

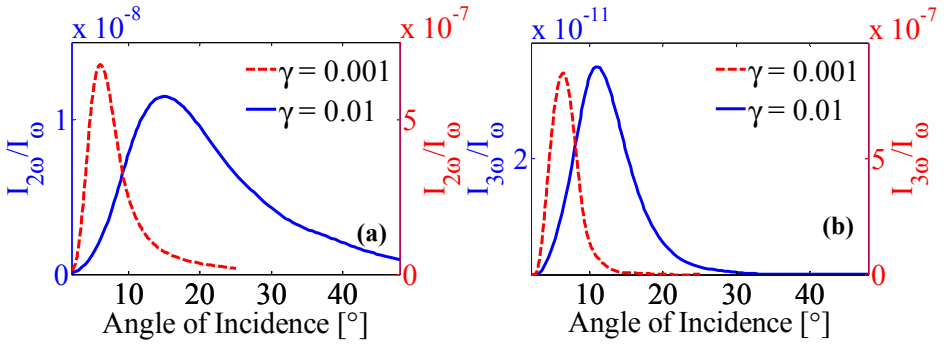

Fig. 5. (a) SH efficiency vs. angle of incidence for a slab d = 200 nm thick, modeled with $\omega_{p1} = \omega_{p2} = \omega_{p3} = 0.906049\,\omega_r$, $\omega_{01} = 0.25\,\omega_r$, $\omega_{02} = 1.652\,\omega_r$, $\omega_{03} = 2.678\,\omega_r$ $\gamma_1 = \gamma_2 = \gamma_3 = 0.01\,\omega_r$ (blue, solid line) and $\gamma_1 = \gamma_2 = \gamma_3 = 0.001\,\omega_r$ (red, dashed line); (b) Same as in (a) for TH.

5. Conclusions

We have discussed SHG and THG in slabs of material with near-zero permittivity. We showed that losses can dramatically influence the nonlinear response in the presence or absence of bulk nonlinearities. If bulk nonlinearities are sufficiently small or absent nonlinear surface, magnetic, and quadrupolar sources cannot be neglected, especially if crossing points are engineered at the harmonic wavelengths. Our findings suggest that sub-wavelength slabs of low-permittivity materials or plasmas may be effectively used to achieve efficient harmonic generation even at low intensities and in the presence of weak nonlinearities.

Acknowledgments

This research was performed while the authors M. A. Vincenti and D. de Ceglia held a National Research Council Research Associateship awards at US Army - AMRDEC.

#197602 - $15.00 USD Received 12 Sep 2013; revised 15 Oct 2013; accepted 16 Oct 2013; published 27 Nov 2013